# Supporting Information

## Inglis et al. 10.1073/pnas.1319334110

### SI Text

**Measurements of $T_1$ for Blood.** *Subject and subject positioning.* MR data were obtained from a healthy man (age 44) using a protocol approved by the Human Subjects Committees of the Lawrence Berkeley National Laboratory and University of California, Berkeley. Informed consent was obtained from the subject. This subject was preferred over the two subjects used for brain imaging because the cephalic veins of his forearms were straight over more than 76 mm, the diameter of the gradiometer pickup loop (Fig. S1). The subject was thus able to position his forearm so that a frequency-encoding gradient applied orthogonal to the cephalic vein projected all of the blood into a narrow frequency band, with minimal contamination from s.c. fat or other arm tissues.

*Two-dimensional imaging of the forearm.* We used 2D imaging to assess our ability to localize a blood signal given the gradiometer geometry and a judicious placement of the arm. As before, $G_{\text{freq}} = 90$ μT/m, and we incremented $G_{\text{phase}}$ in steps of 6.99 μT/m to a maximum value of 105 μT/m. Fig. S2*A* shows a 2D section of the forearm obtained with a single spin echo imaging sequence. Table S1, row 1, lists the acquisition parameters. The major components of the forearm are cortical (hard) bone, bone marrow, muscle, s.c. fat, and blood. Cortical bone, with its low water content and short $T_2$, is not seen. Furthermore, despite its high water content, we could not image muscle because of its short $T_2$ compared with $t_{\text{E1}} = 74$ ms. Thus, Fig. S2*A* is dominated by signals from s.c. fat and marrow in the medullary cavities of the radial and ulna bones, and from blood.

The high fat content of bone marrow and the similarity of $T_1^{B0}$ and $T_1^{Bp}$ for marrow and s.c. fat allow us to use an inversion recovery (IR) imaging sequence to eliminate these signals simultaneously. An inversion recovery imaging sequence set to null fat (see Table S1, row 2, for acquisition parameters) is thus dominated by blood (Fig. S2*B*); in particular, the cephalic vein appears as a bright circle and confirms the projection of the venous signal into a single location of the 2D imaging plane via the geometry of the arm placement.

***$T_1^{B0}$(blood).*** The localization of the cephalic vein in Fig. S2*B* demonstrates that some blood signal is available for measurements and that 1D localization with a frequency-encoding gradient should be sufficient to ensure minimal contamination, once fat signals are eliminated. We therefore measured $T_1^{B0}(blood)$ using a 1D inversion recovery sequence (see Table S1, row 3, for acquisition parameters) with the IR timing chosen to null fat and marrow signals. The values for $t_{T1}^{B0}$ were varied approximately logarithmically using 18 values in the range 18–658 ms. Because of some residual signal from fat, the entire 1D profile was fitted to a double exponential function, yielding $T_1^{B0}(blood) = 190 \pm 39$ ms. The relatively large error probably results from the low signal-to-noice ratio (SNR) available from the small blood volume, but it may also be enhanced by blood flow during the $t_{T1}^{B0}$ array.

***$T_1^{Bp}$(blood).*** Measuring $T_1^{Bp}$ with an array of polarizing pulse durations is incompatible with the use of inversion recovery to null the s.c. fat and bone marrow signals. Thus, 1D localization is insufficient to measure $T_1^{Bp}(blood)$ because of contaminating fat and marrow signals at all polarizing durations. Instead, to obtain $T_1^{Bp}(blood)$, we used a 2D IR imaging sequence to obtain a 2D map. We set an empirical blood null to estimate $T_1^{Bp}$, noting that blood signal passes through a null according to Eq. **1**. Table S1, row 4, lists the acquisition parameters. With $t_{Bp} = 400$ ms and $t^{IR} = 53$ ms, and using the value $T_1^{B0}(blood) = 190 \pm 39$ ms, we estimated $T_1^{Bp}(blood)$ to be ∼450 ms based on the best null for blood in the cephalic vein (Fig. S2*C*). This value for $T_1^{Bp}(blood)$ should be considered an apparent $T_1$, however, because its accuracy is limited to some extent by blood flow. The actual value of $B_p$ experienced by the blood during the pulse sequence changes slightly as a result, varying by ∼10% over the distance from the hand to the forearm—comparable to the path length of the venous blood during a 1- to 2-s imaging sequence.

**Two-Dimensional Brain Imaging.** The set of coronal head images of subject B shown in Fig. S3 was obtained with precisely the same set of acquisition parameters (Table 1, row 3) used to image subject A (Fig. 4). The similarity of the two sets of images is striking.

**Fig. S1.** Forearm prepared for imaging. The subject stood in front of the polarizing coil with his forearm, restrained by memory foam, on a piece of plywood placed on top of the polarizing coil. The front edge of the dewar (indicated by marker pen arc) was used to locate a straight section of cephalic vein directly under the gradiometer (indicated by marker pen dots). The arm placement was adjusted so that the linear section of cephalic vein was oriented parallel to the *y* axis of the system.

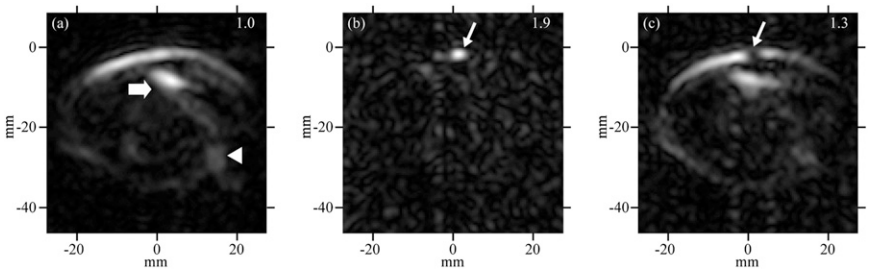


**Fig. S2.** Images of the forearm. (*A*) Spin echo image. Solid arrow, medullary cavity of the radial bone; arrowhead, medullary cavity of the ulna. (*B*) IR image with null set for fat and bone marrow. Arrow, cephalic vein. (*C*) IR image nulling out blood. Arrow, cephalic vein. Image intensities for *B* and *C* are scaled by 1.9 and 1.3, respectively, compared with that for *A*.

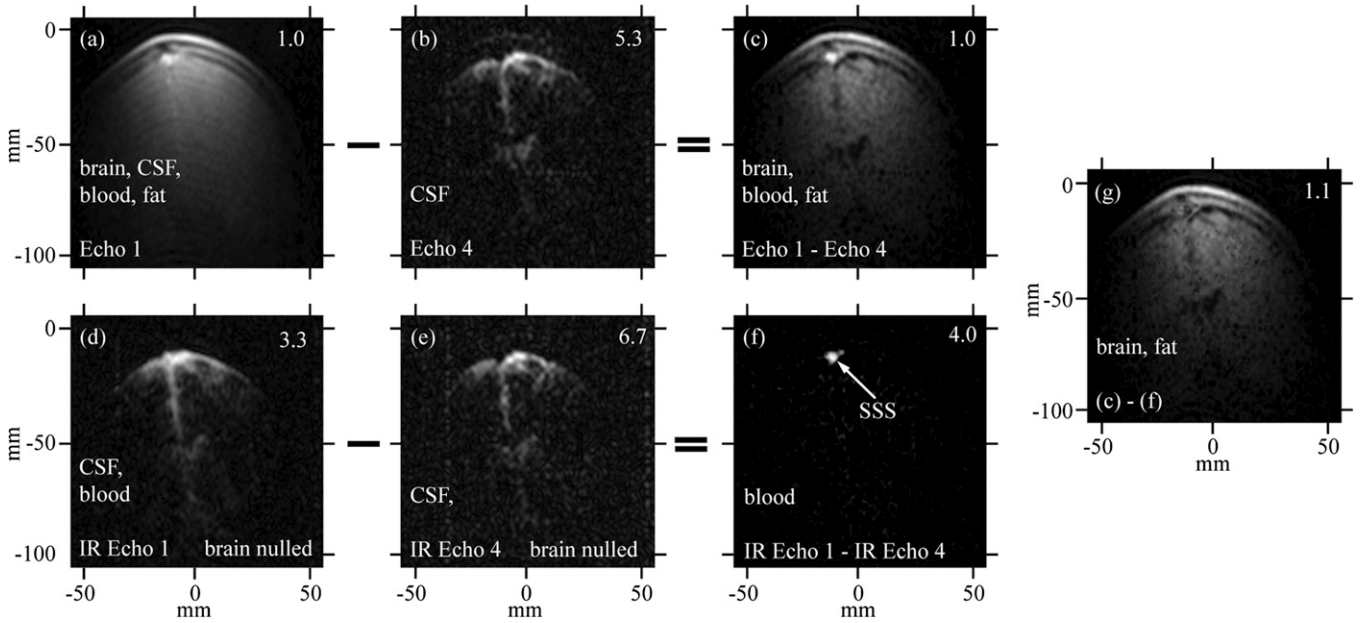


**Fig. S3.** Subject B: 2D brain images. Data acquired using an acquisition of a CPMG sequence (*A* and *B*) interleaved with an IR-CPMG sequence (*D* and *E*) with the inversion recovery delays adjusted to establish a signal null for brain tissue. Values of $T_1$ used to calculate the IR sequence are listed in Table 2. *C* and *F* are obtained from the subtractions $A - B$ and $D - E$, respectively. *G* is the subtraction $C - F$. Image amplitudes have been scaled to enhance visualization of features; scaling factors are given in the top-right corner of each image. The nominal in-plane resolution is 2.5 mm ($z$) × 1.9 mm ($x$). The total imaging time was 25 min, 52 s. Frequency and phase encoding directions are along the $z$ and $x$ axes, respectively.

**Table S1. Parameters for four pulse sequences for the arm**

| Row | Sequence | $t_{Bp}$ (ms) | $t^{IR}$ (ms) | $t^{IR}_{Bp}$ (ms) | $t^{B0}_{T1}$ (ms) | $t_{E1}$ (ms) | $t_{E2}$ (ms) | No. echoes | No. averages | No. PE steps | PE resolution (mm) | FE resolution (mm) | Acquisition time |
|---|---|---|---|---|---|---|---|---|---|---|---|---|---|
| 1 | SE | 500 | — | — | 18 | 74 | — | 1 | 1 | 31 | 2.5 | 2.5 | 1 min, 12 s |
| 2 | IR SE | 500 | 70 | 75 | 18 | 74 | — | 1 | 2 | 31 | 2.5 | 2.5 | 2 min, 44 s |
| 3 | IR SE | 500 | 53 | 90 | 18–658 | 74 | — | 1 | 8 | — | — | 2.5 | 7 min, 52 s |
| 4 | IR SE | 400 | 53 | 170 | 18 | 74 | — | 1 | 2 | 31 | 2.5 | 2.5 | 3 min, 23 s |

Row 1, 2D spin echo sequence to acquire forearm cross section; row 2, 2D IR spin echo sequence to acquire forearm fat-nulled image; row 3, 1D IR sequence to acquire $T_1^{B0}(blood)$; row 4, 2D IR sequence to null the blood and thereby estimate $T_1^{Bp}(blood)$. SE, spin echo; FE, frequency encoding; PE, phase encoding.